

Klimaänderung I

4. Das zukünftige globale Klima: Szenarien-basierte Projektionen und kurzfristiger Ausblick

Robert Sausen

Institut für Physik der Atmosphäre
Deutsches Zentrum für Luft- und Raumfahrt
Oberpfaffenhofen

Vorlesung WS 2021/22

LMU München



Knowledge for Tomorrow

Technical information

- <http://www.pa.op.dlr.de/~RobertSausen/vorlesung/index.html>
 - Most recent update on the lecture
 - Slides of the lecture (with some delay)

 - See also LSF <https://lsf.verwaltung.uni-muenchen.de/>

- Contact: robert.sausen@dlr.de

- Further information:
 - www.ipcc.ch
 - www.de-ipcc.de



Contents of IPCC AR 6 2021

Working Group I: the Physical Science Basis

Chapters	
Chapter 1: Framing, context, methods	DOWNLOAD
Chapter 2: Changing state of the climate system	DOWNLOAD
Chapter 3: Human influence on the climate system	DOWNLOAD
Chapter 4: Future global climate: scenario-based projections and near-term information	DOWNLOAD
Chapter 5: Global carbon and other biogeochemical cycles and feedbacks	DOWNLOAD
Chapter 6: Short-lived climate forcers	DOWNLOAD
Chapter 7: The Earth's energy budget, climate feedbacks, and climate sensitivity	DOWNLOAD
Chapter 8: Water cycle changes	DOWNLOAD
Chapter 9: Ocean, cryosphere, and sea level change	DOWNLOAD
Chapter 10: Linking global to regional climate change	DOWNLOAD
Chapter 11: Weather and climate extreme events in a changing climate	DOWNLOAD
Chapter 12: Climate change information for regional impact and for risk assessment	DOWNLOAD
Atlas	DOWNLOAD
Supplementary Material	▼
Annexes	▼

<https://www.ipcc.ch/report/ar6/wg1/#FullReport>



Chapter 4: Future global climate: scenario-based projections and near-term information

Coordinating Lead Authors:

June-Yi Lee (Republic of Korea), **Jochem Marotzke (Germany)**

Lead Authors:

Govindasamy Bala (India/United States of America), Long Cao (China), Susanna Corti (Italy), John P. Dunne (United States of America), Francois Engelbrecht (South Africa), Erich Fischer (Switzerland), John C. Fyfe (Canada), Christopher Jones (United Kingdom), Amanda Maycock (United Kingdom), Joseph Mutemi (Kenya), Ousmane Ndiaye (Senegal), Swapna Panickal (India), Tianjun Zhou (China)

Chapter 3: Human influence on the climate system

Contributing Authors:

Sebastian Milinski (Germany), Kyung-Sook Yun (Republic of Korea), Kyle Armour (United States of America), Nicolas Bellouin (United Kingdom/France), Ingo Bethke (Norway/Germany), Michael P. Byrne (United Kingdom /Ireland), Christophe Cassou (France), Deliang Chen (Sweden), Annalisa Cherchi (Italy), Hannah M. Christensen (United Kingdom), Sarah L. Connors (France/United Kingdom), Alejandro Di Luca (Australia, Canada/Argentina), Sybren S. Drijfhout (The Netherlands), Christopher G. Fletcher (Canada/United Kingdom, Canada), Piers Forster (United Kingdom), Javier García-Serrano (Spain), Nathan P. Gillett (Canada), Darrell S. Kaufmann (United States of America), David P. Keller (Germany/United States of America), Ben Kravitz (United States of America), Hongmei Li (Germany/China), Yongxiao Liang (Canada/China), Andrew H. MacDougall (Canada), Elizaveta Malinina (Canada/Russian Federation), Matthew Menary (France/United Kingdom), William J. Merryfield (Canada/United States of America), Seung-Ki Min (Republic of Korea), Zebedee R.J. Nicholls (Australia), **Dirk Notz (Germany)**, Brodie Pearson (United States of America/United Kingdom), Matthew D. K. Priestley (United Kingdom), **Johannes Quaas (Germany)**, Aurélien Ribes (France), Alex C. Ruane (United States of America), Jean-Baptiste Sallée (France), Emilia Sanchez-Gomez (France/Spain), Sonia I. Seneviratne (Switzerland), Aimée B. A. Slangen (The Netherlands), Chris Smith (United Kingdom), Malte F. Stuecker (United States of America/Germany), Ranjini Swaminathan (United Kingdom/India), Peter W. Thorne (Ireland/ United Kingdom), Katarzyna B. Tokarska (Switzerland/Poland), **Matthew Toohey (Canada, Germany/Canada)**, Andrew Turner (United Kingdom), Danila Volpi (Italy), Cunde Xiao (China), Giuseppe Zappa (Italy)

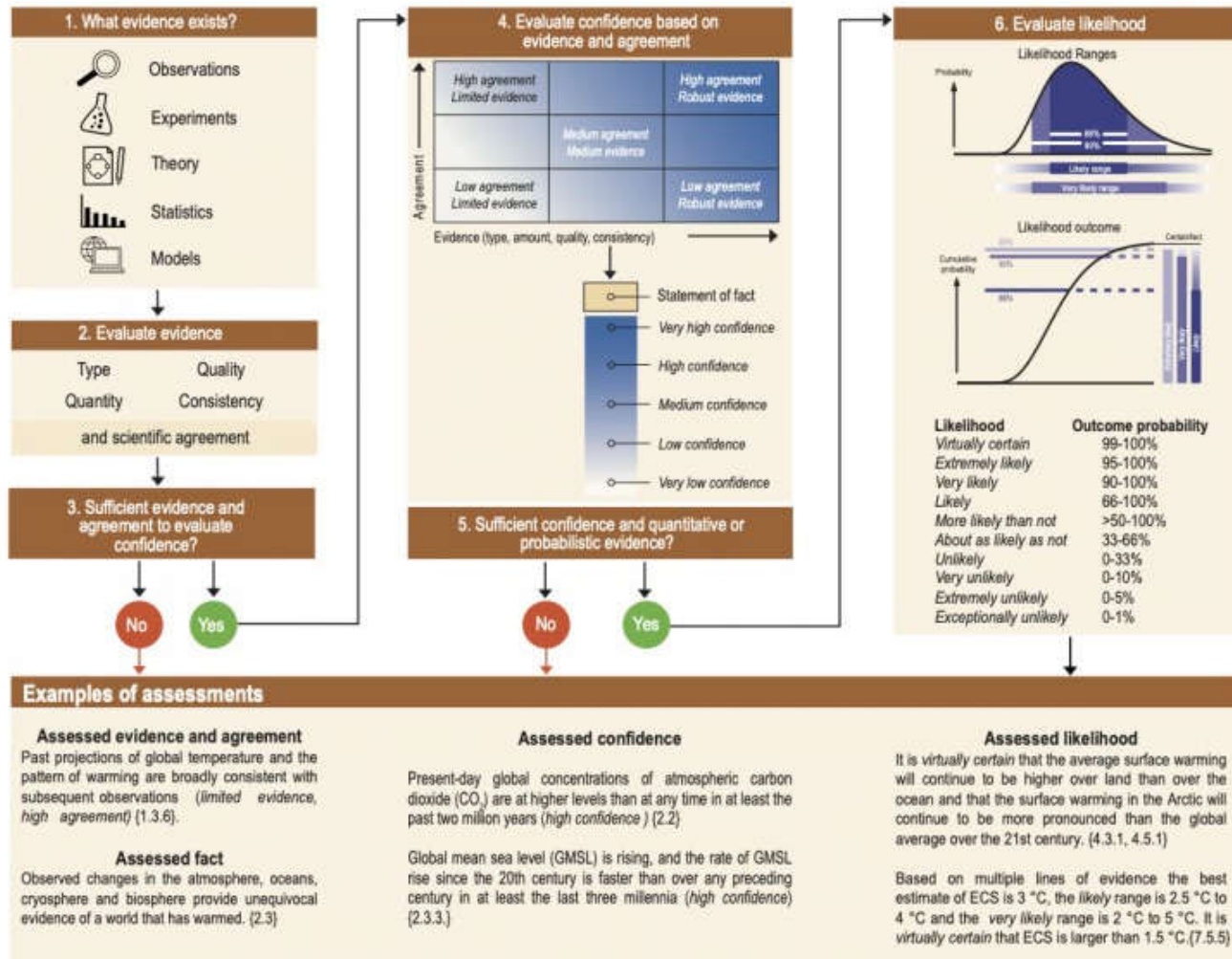
Review Editors:

Krishna Kumar Kanikicharla (Qatar/India), Vladimir Kattsov (Russian Federation), Masahide Kimoto (Japan)



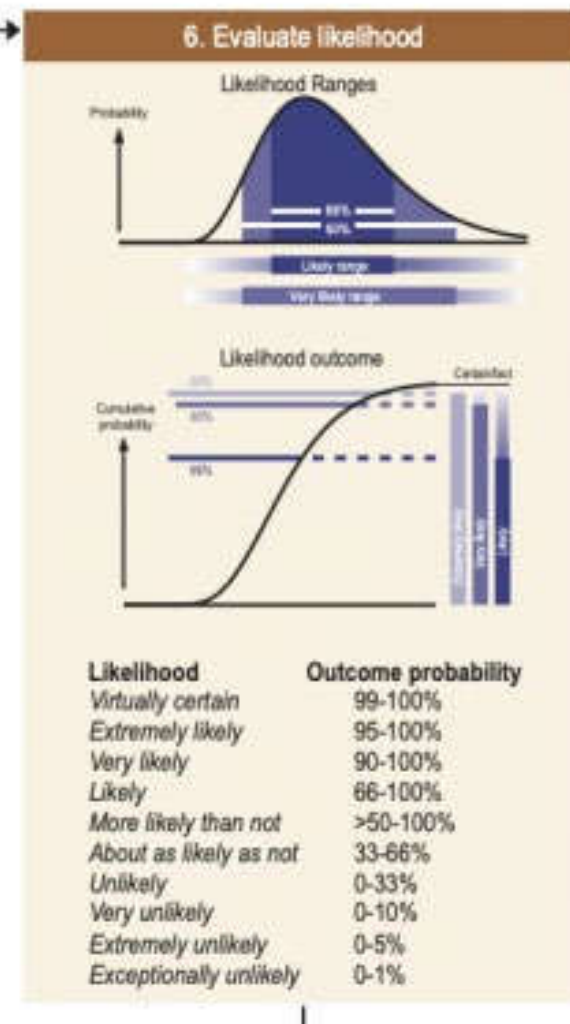
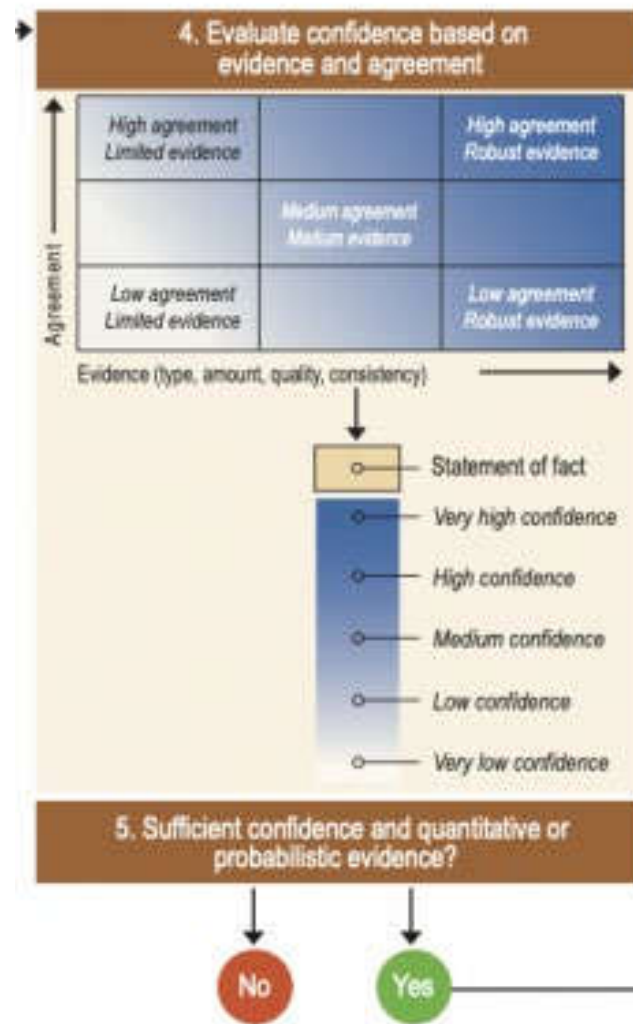
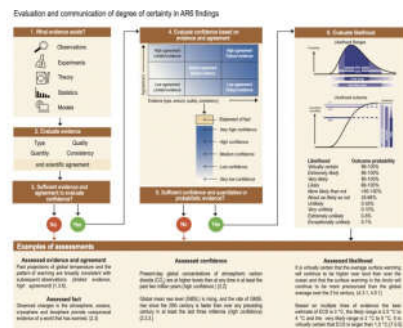


Evaluation and communication of degree of certainty in AR6 findings





IPCC 2021, Chap. 1



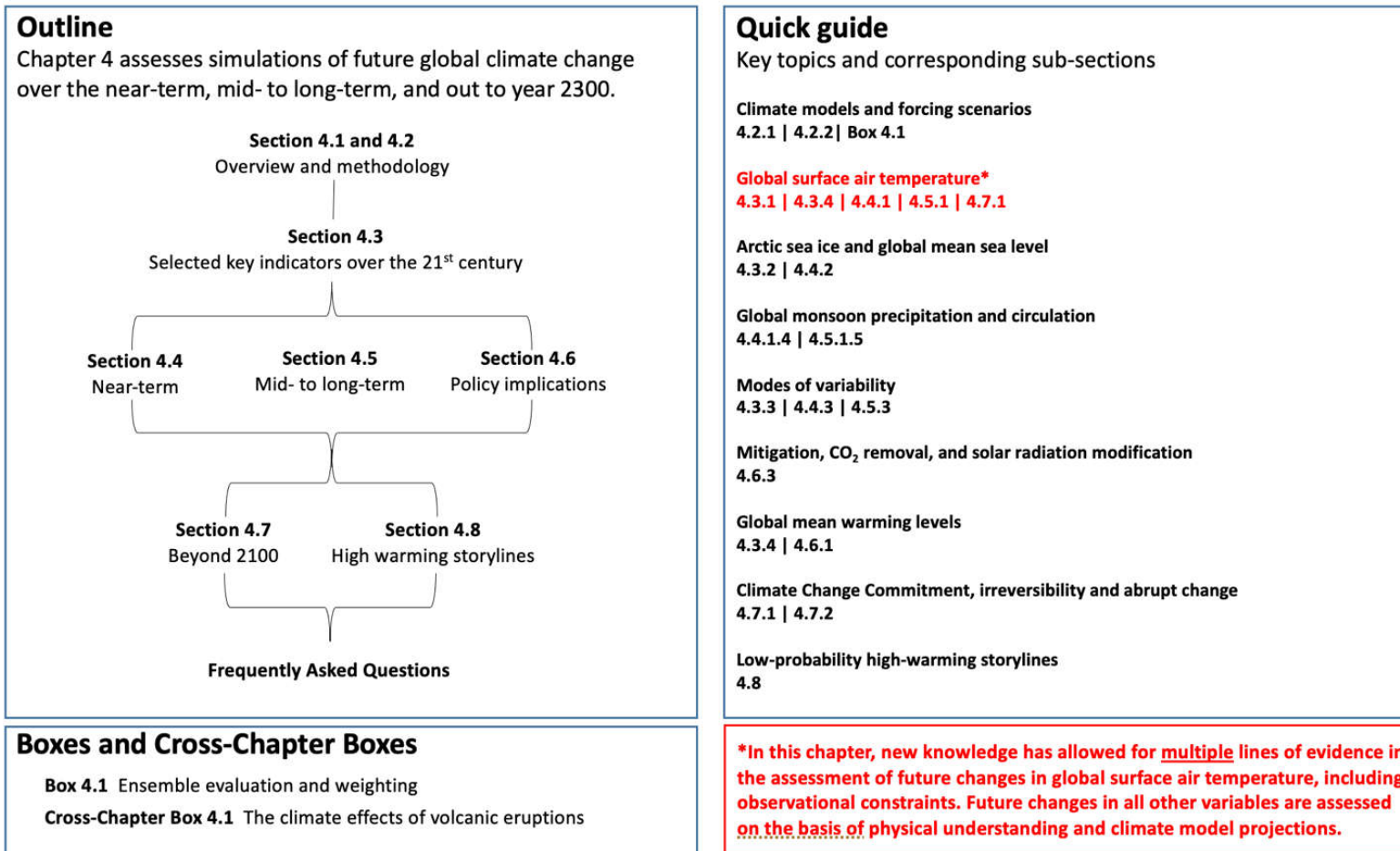


Figure 4.1: Visual abstract of Chapter 4. The chapter outline and a quick guide for key topics and corresponding subsections are provided.



Statements in the Executive Summary

This chapter assesses simulations of future global climate change, spanning time horizons from the near term (2021–2040), mid-term (2041–2060), and long term (2081–2100) out to the year 2300. Changes are assessed relative to both the recent past (1995–2014) and the 1850–1900 approximation to the pre-industrial period.

The projections assessed here are mainly based on a new range of scenarios, the Shared Socio-economic Pathways (SSPs) used in the Coupled Model Intercomparison Project Phase 6 (CMIP6). Among the SSPs, the focus is on the five scenarios SSP1-1.9, SSP1-2.6, SSP2-4.5, SSP3-7.0, and SSP5-8.5. In the SSP labels, the first number refers to the assumed shared socio-economic pathway, and the second refers to the approximate global effective radiative forcing (ERF) in 2100. Where appropriate, this chapter also assesses new results from CMIP5, which used scenarios based on Representative Concentration Pathways (RCPs). Additional lines of evidence enter the assessment, especially for change in globally averaged surface air temperature (GSAT) and global mean sea level (GMSL), while assessment for changes in other quantities is mainly based on CMIP6 results. Unless noted otherwise, the assessments assume that there will be no major volcanic eruption in the 21st century. {1.6, 4.2.2, 4.3.2, 4.3.4, 4.6.2, BOX 4.1: Cross-17 Chapter Box 4.1, Cross-Chapter Box 7.1, 9.6}

Statements in the Executive Summary

Temperature (1)

Assessed future change in GSAT is, for the first time in an IPCC report, explicitly constructed by combining scenario-based projections with observational constraints based on past simulated warming, as well as an updated assessment of equilibrium climate sensitivity (ECS) and transient climate response (TCR). Climate forecasts initialized using recent observations have also been used for the period 2019–2028. The inclusion of additional lines of evidence has reduced the assessed uncertainty ranges for each scenario. {4.3.1, 4.3.4, 4.4.1, 7.5}



Statements in the Executive Summary

Temperature (2a)

In the near term (2021–2040), a 1.5°C increase in the 20-year average of GSAT, relative to the average over the period 1850–1900, is *very likely* to occur in scenario **SSP5-8.5**, *likely* to occur in scenarios **SSP2-4.5** and **SSP3-7.0**, and *more likely than not* to occur in scenarios **SSP1-1.9** and **SSP1-2.6**. The threshold-crossing time is defined as the midpoint of the first 20-year period during which the average GSAT exceeds the threshold. In all scenarios assessed here except SSP5-8.5, the central estimate of crossing the 1.5°C threshold lies in the early 2030s. This is about ten years earlier than the midpoint of the *likely* range (2030–2052) assessed in the SR1.5, which assumed continuation of the then-current warming rate; this rate has been confirmed in the AR6. Roughly half of the ten-year difference between assessed crossing times arises from a larger historical warming diagnosed in AR6. ...

SR1.5



IPCC 2021, Chap. 4



Statements in the Executive Summary

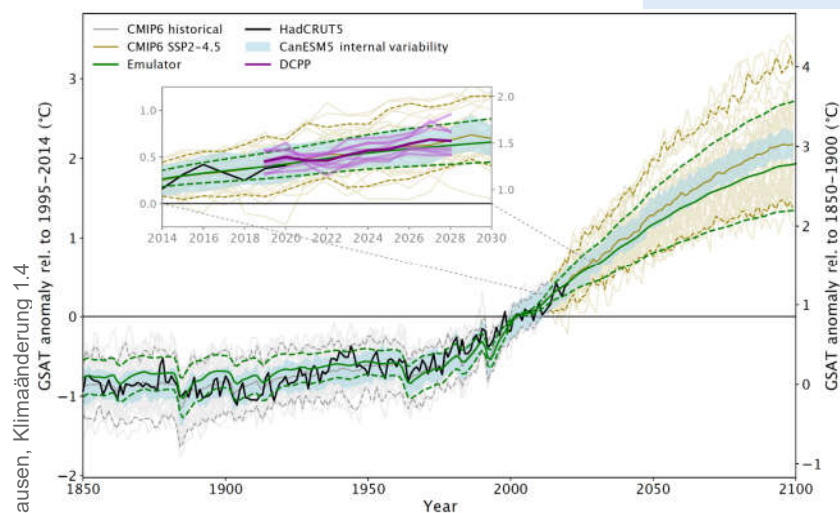
Temperature (2b)

... The other half arises because for central estimates of climate sensitivity, most scenarios show stronger warming over the near term than was assessed as 'current' in SR1.5 (*medium confidence*). It is *more likely than not* that under SSP1-1.9, GSAT relative to 1850–1900 will remain below 1.6°C throughout the 21st century, implying a potential temporary overshoot of 1.5°C global warming of no more than 0.1°C. If climate sensitivity lies near the lower end of the assessed *very likely* range, crossing the 1.5°C warming threshold is avoided in scenarios SSP1-1.9 and SSP1-2.6 (*medium confidence*). {2.3.1, Cross-chapter Box 2.3, 3.3.1, 4.3.4, BOX 4.1:, 7.5}



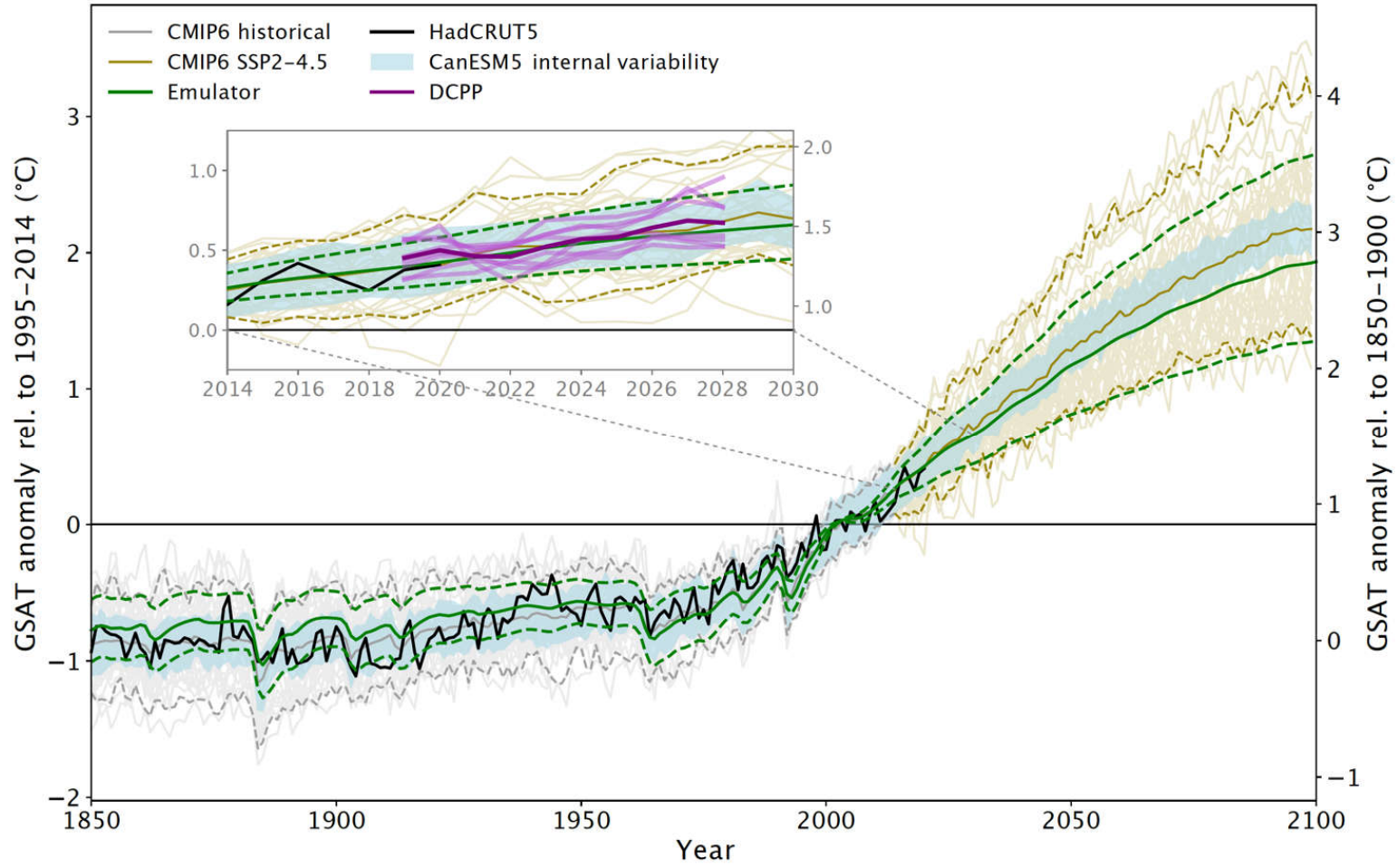
CMIP6 annual-mean GSAT simulations and various contributions to uncertainty in the projections ensemble

Box 4.1 Figure 1: CMIP6 annual-mean GSAT simulations and various contributions to uncertainty in the projections ensemble. The figure shows anomalies relative to the period 1995–2014 (left y-axis), converted to anomalies relative to 1850–1900 (right y-axis); the difference between the y-axes is 0.85°C (Cross-Chapter Box 2.3). Shown are historical simulations with 39 CMIP6 models (grey) and projections following scenario SSP2-4.5 (dark yellow; thin lines: individual simulations; heavy line; ensemble mean; dashed lines: 5% and 95% ranges). The black curve shows the observations-based estimate (HadCRUT5, (Morice et al., 2021)). Light blue shading shows the 50-member ensemble CanESM5, such that the deviations from the CanESM5 ensemble mean have been added to the CMIP6 multi-model mean. The green curves are from the emulator and show the central estimate (solid) and *very likely* range (dashed) for GSAT. The inset shows a cut-out from the main plot and additionally in light purple for the period 2019–2028 the initialized forecasts from eight models contributing to DCP (Boer et al., 2016); the deep-purple curve shows the average of the forecasts. Further details on data sources and processing are available in the chapter data table (Table 4.SM.1).



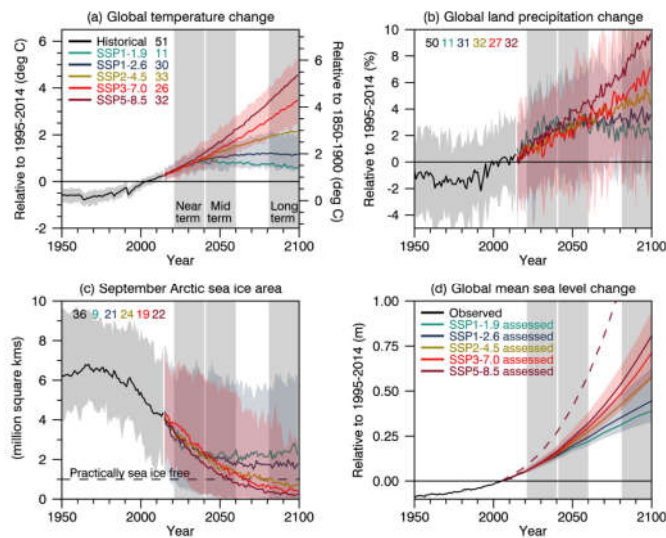


09.02.2022



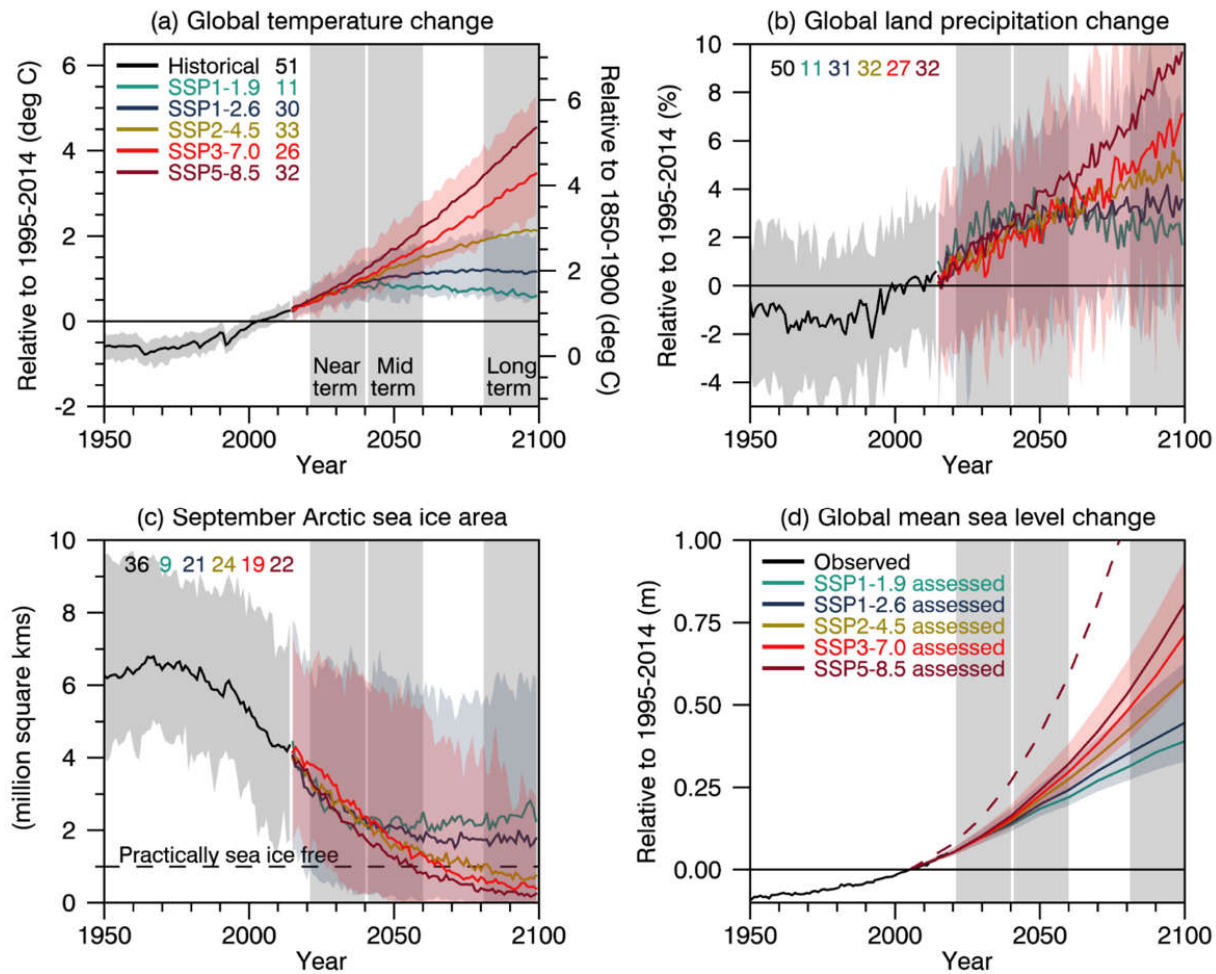
Selected indicators of global climate change from CMIP6 historical and scenario simulations

Figure 4.2: Selected indicators of global climate change from CMIP6 historical and scenario simulations. (a)



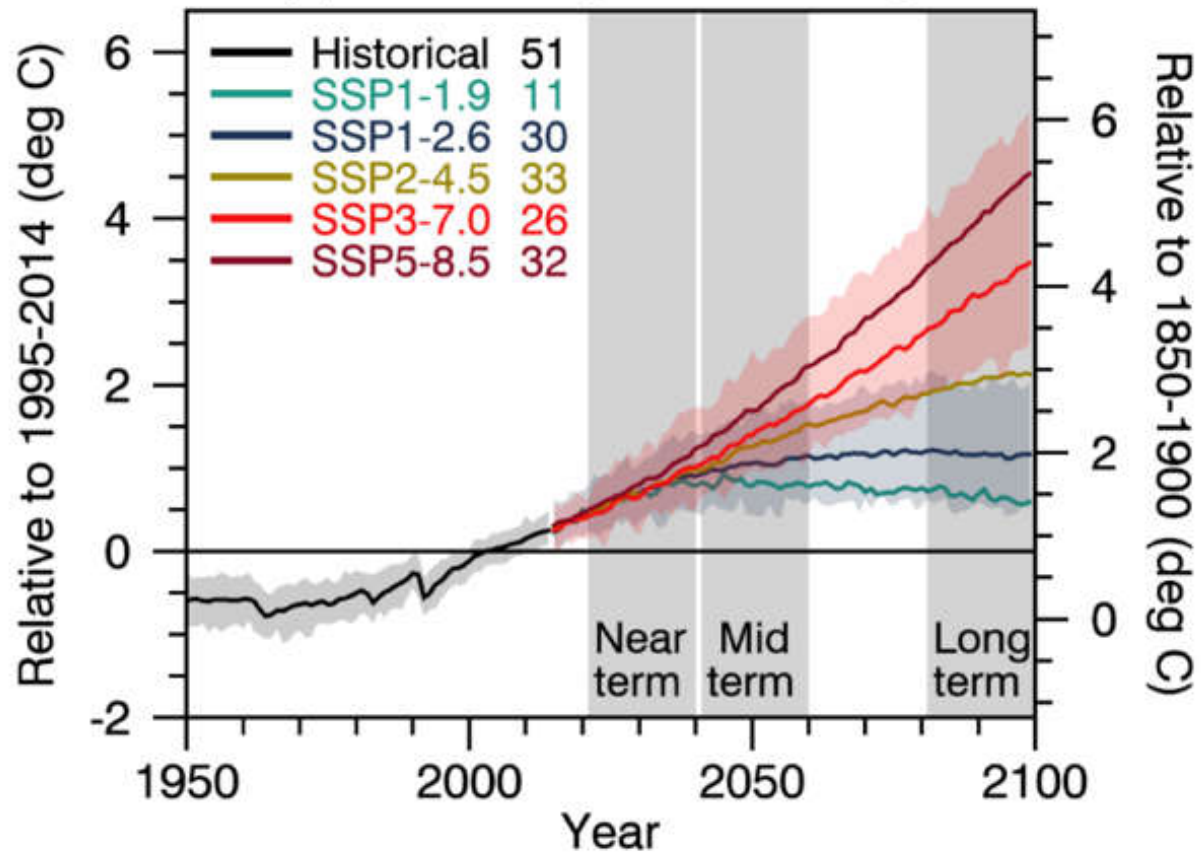
(b) Global land precipitation changes relative to the 1995–2014 average. (c) September Arctic sea-ice area. (d) Global mean sea-level change (GMSL) relative to the 1995–2014 average. (a), (b) and (d) are annual averages, (c) are September averages. In (a)-(c), the curves show averages over the CMIP6 simulations, the shadings around the SSP1-2.6 and SSP3-7.0 curves show 5–95% ranges, and the numbers near the top show the number of model simulations used. Results are derived from concentration-driven simulations. In (d), the barostatic contribution to GMSL (i.e., the contribution from land-ice melt) has been added offline to the CMIP6 simulated contributions from thermal expansion (thermometric). The shadings around the SSP1-2.6 and SSP3-7.0 curves show 5–95% ranges. The dashed curve is the *low confidence* and low likelihood outcome at the high end of SSP5-8.5 and reflects deep uncertainties arising from potential ice-sheet and ice-cliff instabilities. This curve at year 2100 indicates 1.7 m of GMSL rise relative to 1995–2014. More information on the calculation of GMSL are available in Chapter 9, and further regional details are provided in the Atlas. Further details on data sources and processing are available in the chapter data table (Table 4.SM.1).







(a) Global temperature change

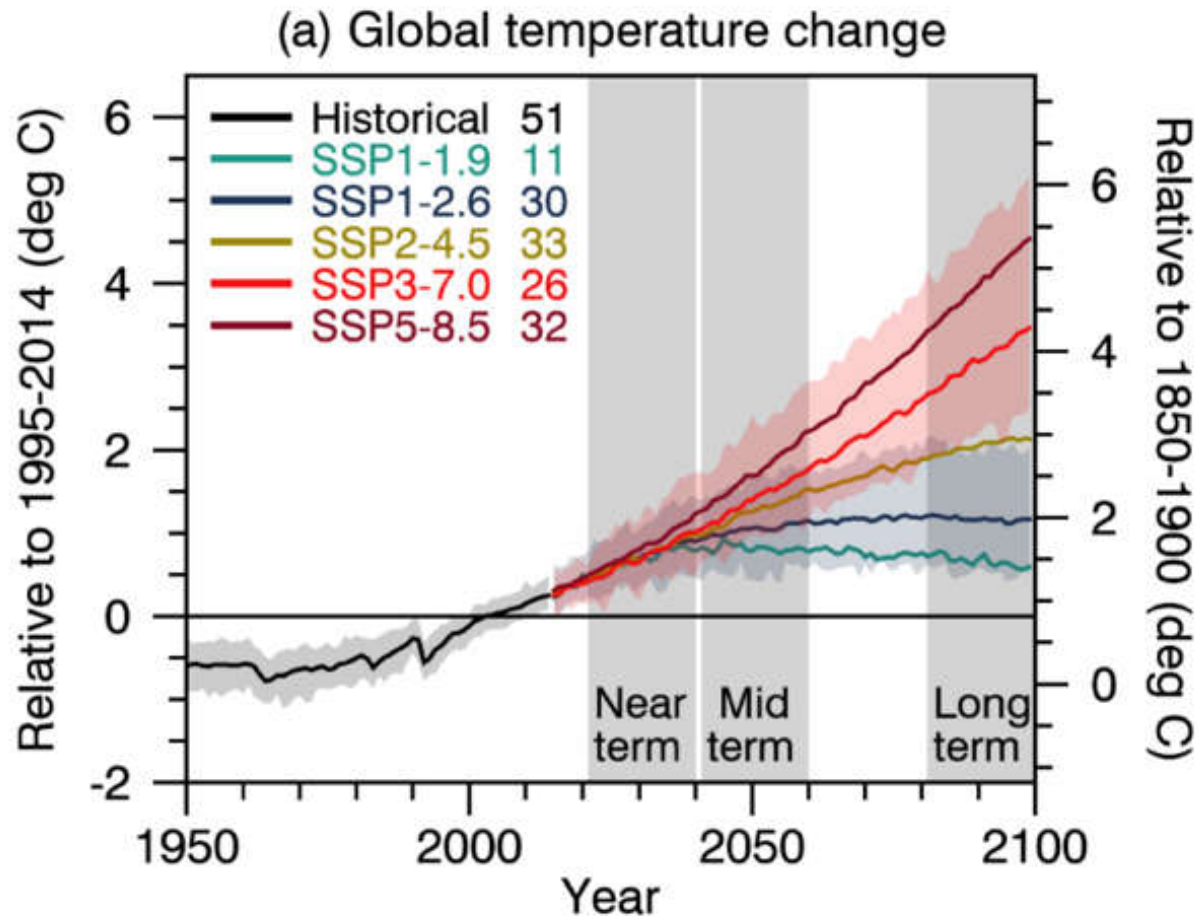


Statements in the Executive Summary

Temperature (3)

By 2030, GSAT in any individual year could exceed 1.5°C relative to 1850–1900 with a likelihood between 40% and 60%, across the scenarios considered here (*medium confidence*). Uncertainty in near-term projections of annual GSAT arises in roughly equal measure from natural internal variability and model uncertainty (*high confidence*). By contrast, near-term annual GSAT levels depend less on the scenario chosen, consistent with the AR5 assessment. Forecasts initialized from recent observations simulate annual GSAT changes for the period 2019–2028 relative to the recent past that are consistent with the assessed *very likely* range (*high confidence*). {4.4.1, BOX 4.1:}





Statements in the Executive Summary

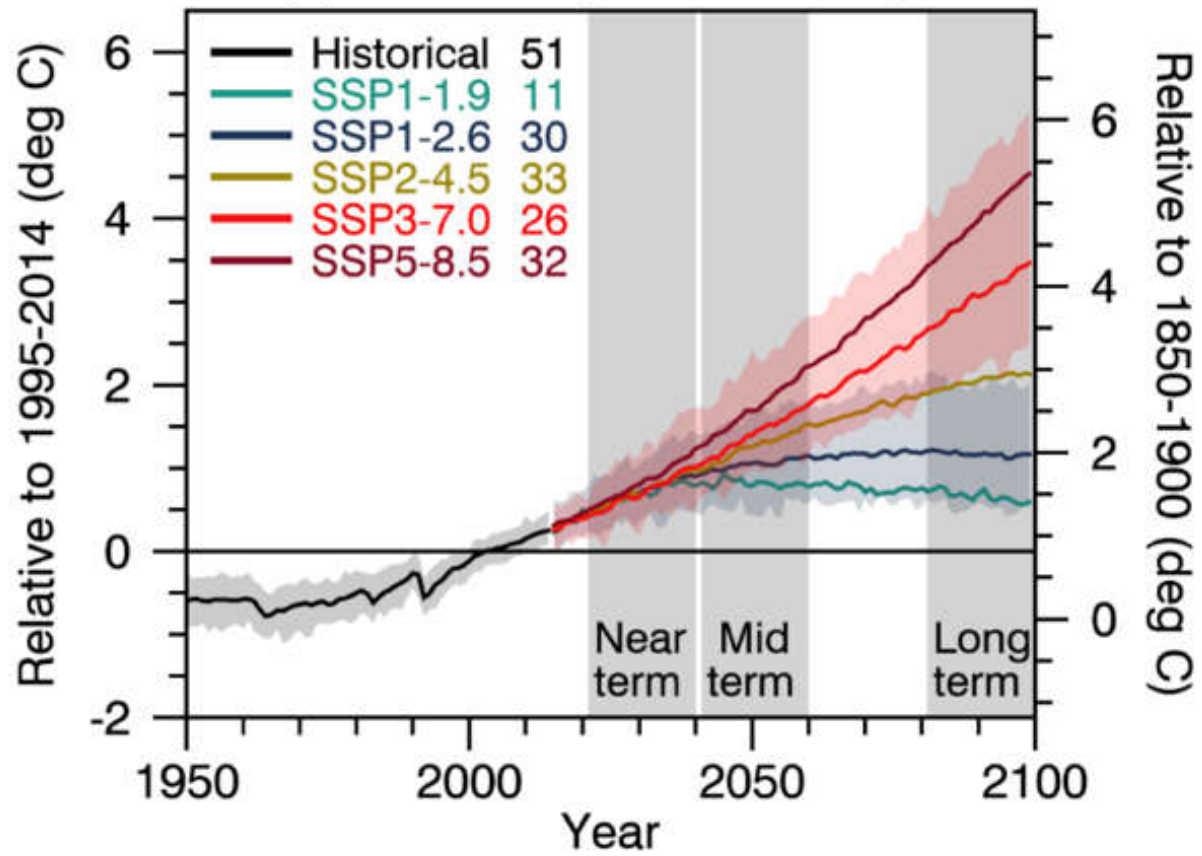
Temperature (4)

Compared to the recent past (1995–2014), GSAT averaged over the period 2081–2100 is *very likely* to be higher by 0.2°C–1.0°C in the low-emission scenario **SSP1-1.9** and by **2.4°C–4.8°C** in the high-emission scenario **SSP5-8.5**. For the scenarios SSP1-2.6, SSP2-4.5, and SSP3-7.0, the corresponding *very likely* ranges are 0.5°C–1.5°C, 1.2°C–2.6°C, and 2.0°C–3.7°C, respectively. The uncertainty ranges for the period 2081–2100 continue to be dominated by the uncertainty in ECS and TCR (*very high confidence*). Emissions-driven simulations for SSP5-8.5 show that carbon-cycle uncertainty is too small to change the assessment of GSAT projections (*high confidence*). {4.3.1, 4.3.4, 4.6.2, 7.5}





(a) Global temperature change



Comparison of concentration-driven and emission-driven simulation

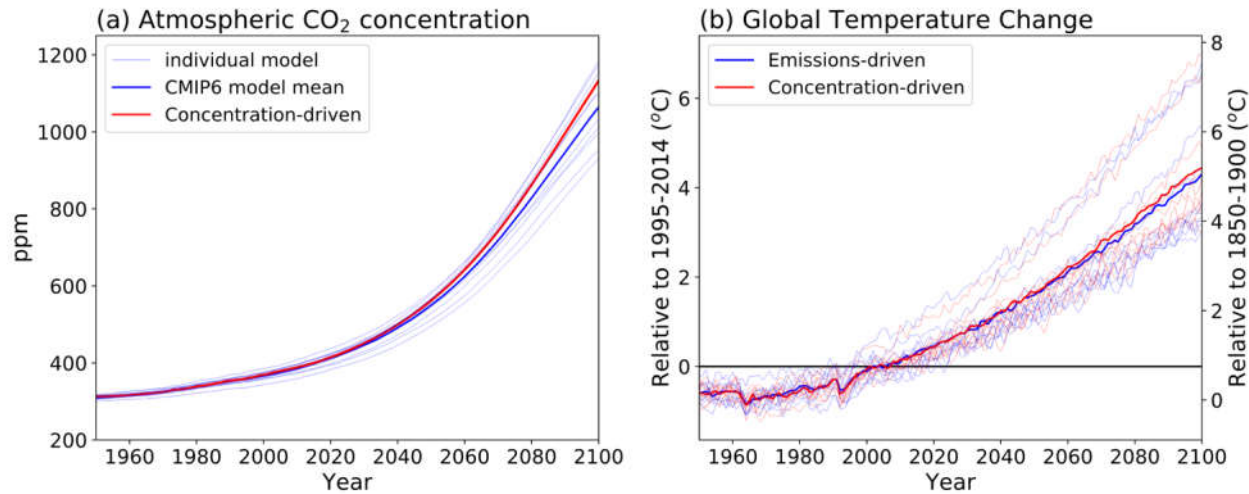
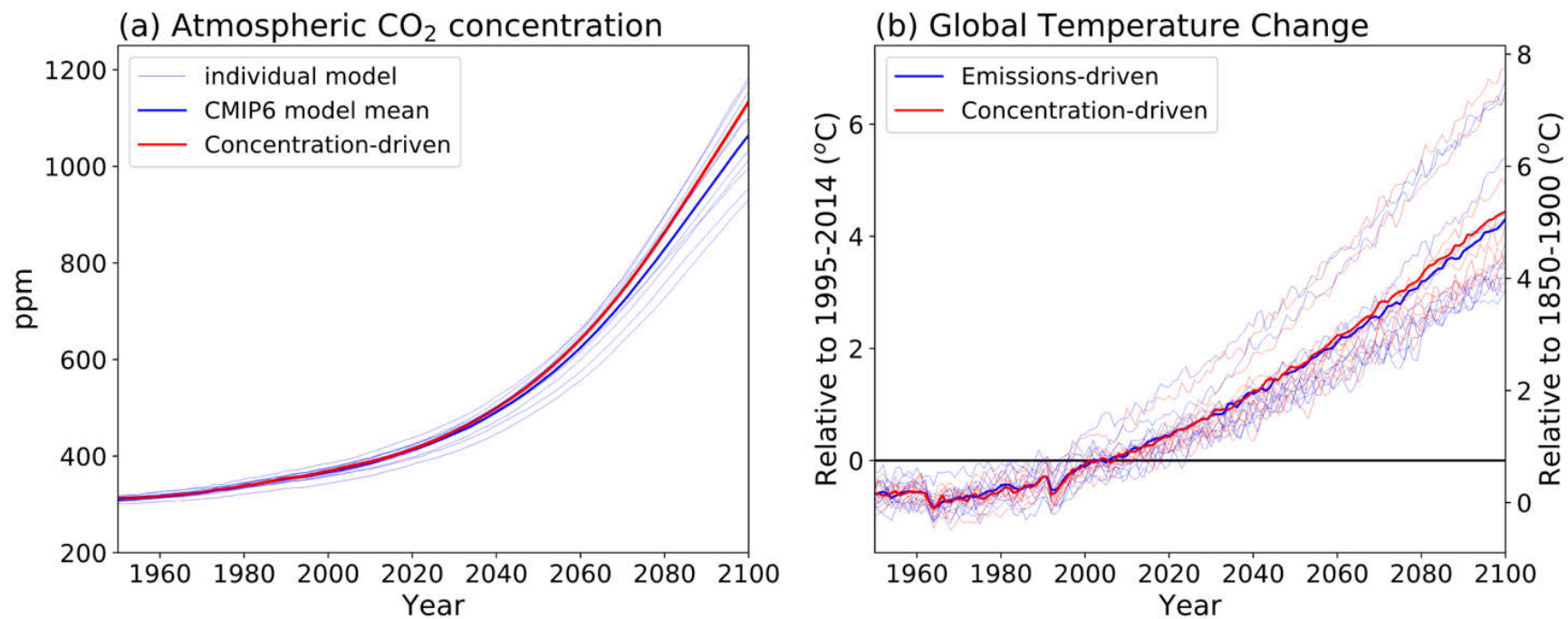


Figure 4.3: Comparison of concentration-driven and emission-driven simulation. (a) Atmospheric CO₂ concentration, (b) GSAT from models which performed SSP5-8.5 scenario simulations in both emissions-driven (blue; *esm-ssp585*) and concentration-driven (red; *ssp585*) configurations. For concentration driven simulations, CO₂ concentration is prescribed, and follows the red line in panel (a) in all models. For emissions-driven simulations, CO₂ concentration is simulated and can therefore differ for each model, blue lines in panel (a). Further details on data sources and processing are available in the chapter data table (Table 4.SM.1).



Comparison of concentration-driven and emission-driven simulation



Statements in the Executive Summary

Temperature (5)

The CMIP6 models project a wider range of GSAT change than the assessed range (*high confidence*); furthermore, the CMIP6 GSAT increase tends to be larger than in CMIP5 (*very high confidence*). About half of the increase in simulated warming has occurred because higher climate sensitivity is more prevalent in CMIP6 than in CMIP5; the other half arises from higher ERF in nominally comparable scenarios (e.g., RCP8.5 and SSP5-8.5; *medium confidence*). In SSP1-2.6 and SSP2-4.5, ERF changes also explain about half of the changes in the range of warming (*medium confidence*). For SSP5-8.5, higher climate sensitivity is the primary reason behind the upper end of the warming being higher than in CMIP5 (*medium confidence*). {4.3.1, 4.3.4, 4.6.2, 7.5.6}



Statements in the Executive Summary

Temperature (6)

While high-warming storylines – those associated with GSAT levels above the upper bound of the assessed *very likely* range – are by definition *extremely unlikely*, they cannot be ruled out. For SSP1-2.6, such a high-warming storyline implies long-term (2081–2100) warming well above, rather than well below, 2° C (*high confidence*).

Irrespective of scenario, high-warming storylines imply changes in many aspects of the climate system that exceed the patterns associated with the central estimate of GSAT changes by up to more than 50% (*high confidence*). {4.3.4, 4.8}



Statements in the Executive Summary

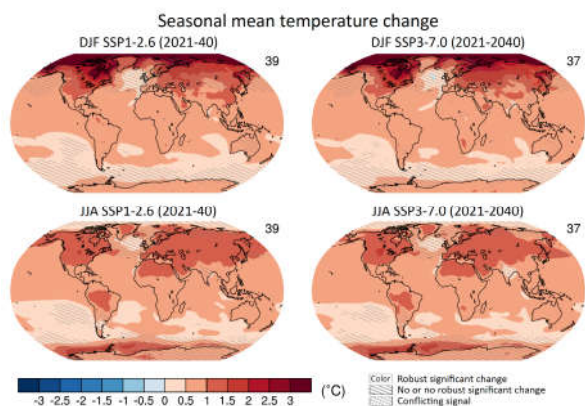
Temperature (7)

It is *virtually certain* that the average surface warming will continue to be higher over land than over the ocean and that the surface warming in the Arctic will continue to be more pronounced than the global average over the 21st century. The warming pattern likely varies across seasons, with northern high latitudes warming more during boreal winter than summer (*medium confidence*). Regions with increasing or decreasing year-to-year variability of seasonal mean temperatures will *likely* increase in their spatial extent. {4.3.1, 4.5.1, 7.4.4}



Near-term change of seasonal mean surface temperature

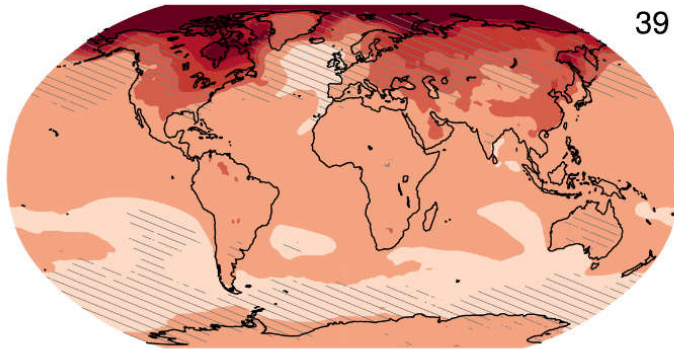
Figure 4.12: Near-term change of seasonal mean surface temperature. Displayed are projected spatial patterns of CMIP6 multi-model mean change ($^{\circ}\text{C}$) in (top) DJF and (bottom) JJA near-surface air temperature for 2021–2040 from SSP1-2.6 and SSP3-7.0 relative to 1995–2014. The number of models used is indicated in the top right of the maps. No overlay indicates regions where the change is robust and *likely* emerges from internal variability, that is, where at least 66% of the models show a change greater than the internal-variability threshold (see Section 4.2.6) and at least 80% of the models agree on the sign of change. Diagonal lines indicate regions with no change or no robust significant change, where fewer than 66% of the models show change greater than the internal-variability threshold. Crossed lines indicate areas of conflicting signals where at least 66% of the models show change greater than the internal-variability threshold but fewer than 80% of all models agree on the sign of change. Further details on data sources and processing are available in the chapter data table (Table 4.SM.1).



Seasonal mean temperature change

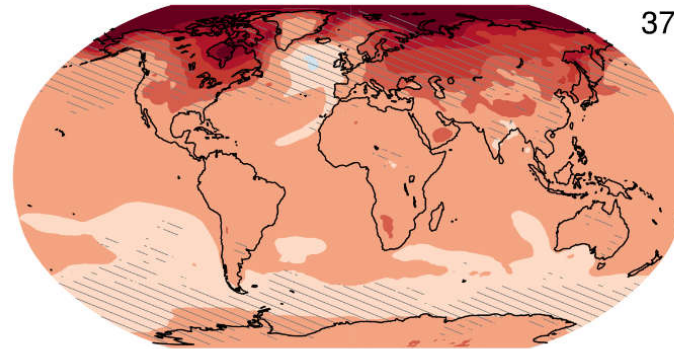
DJF SSP1-2.6 (2021-40)

39



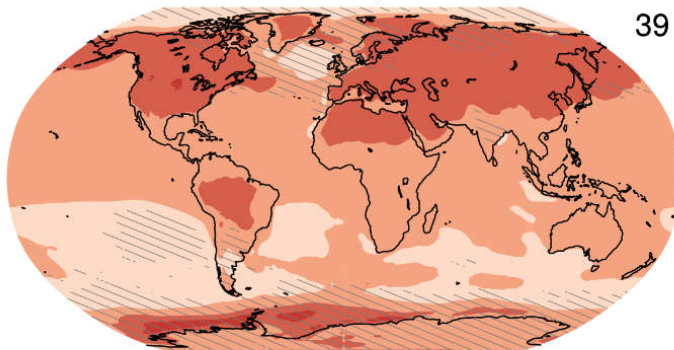
DJF SSP3-7.0 (2021-2040)

37



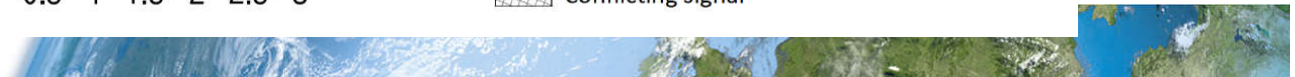
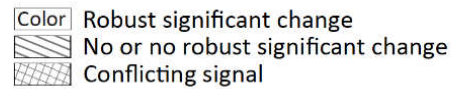
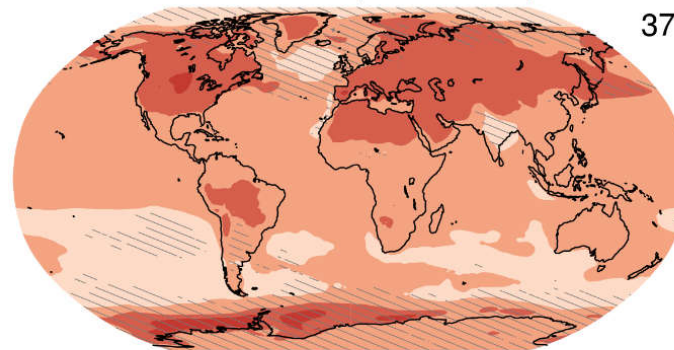
JJA SSP1-2.6 (2021-40)

39



JJA SSP3-7.0 (2021-2040)

37

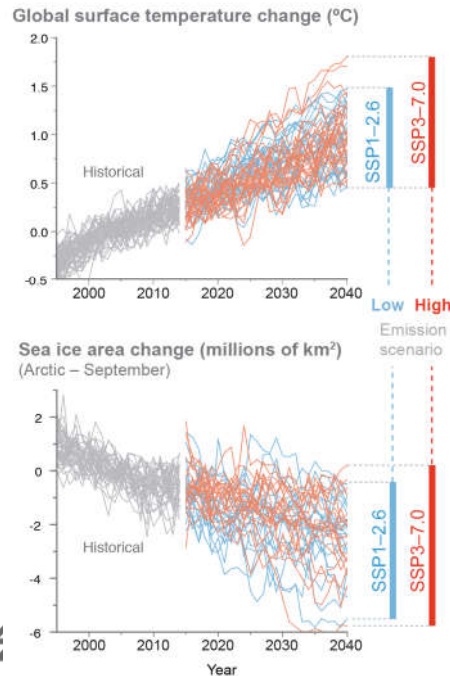


Simulations over the period 1995–2040, encompassing the recent past and the next twenty years, of two important indicators of global climate change

FAQ 4.1, Figure 1: Simulations over the period 1995–2040, encompassing the recent past and the next twenty years, of two important indicators of global climate change. (top) global surface temperature, and (bottom), the area of Arctic sea ice in September. Both quantities are shown as deviations from the average over the period 1995–2014. The black curves are for the historical period ending in 2014; the blue curves represent a low-emission scenario (SSP1-2.6) and the red curves one high-emission scenario (SSP3-7.0).

FAQ 4.1: How will climate change over the next 20 years?

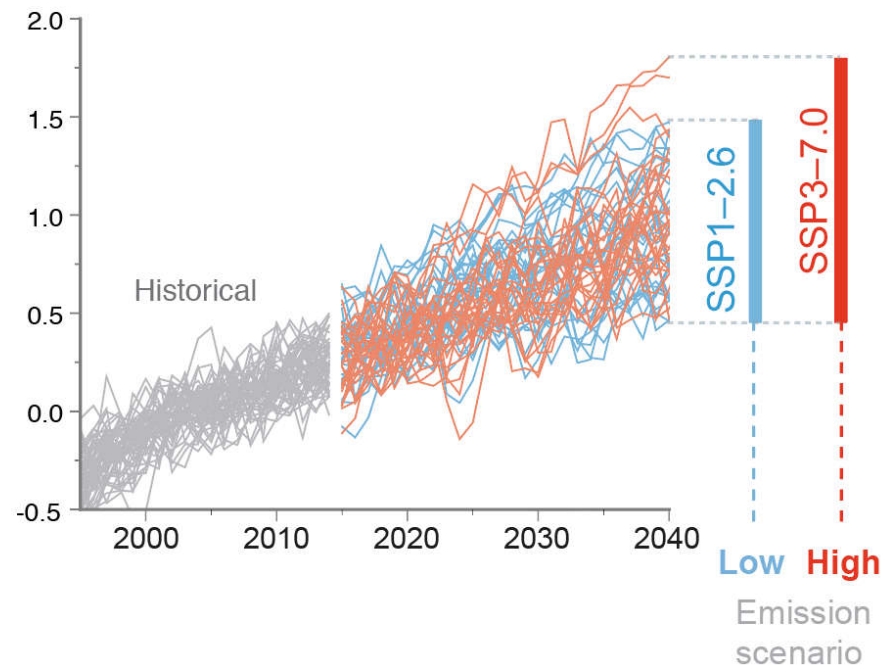
Current climatic trends will continue in the next 2 decades but their exact magnitude cannot be predicted, because of natural variability.



FAQ 4.1: How will climate change over the next 20 years?

Current climatic trends will continue in the next 2 decades but their exact magnitude cannot be predicted, because of natural variability.

Global surface temperature change (°C)

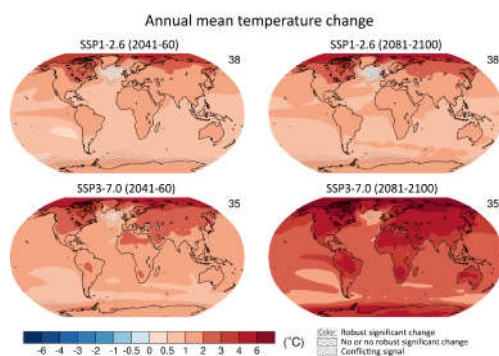


IPCC 2021, Chap. 4

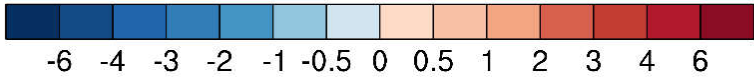
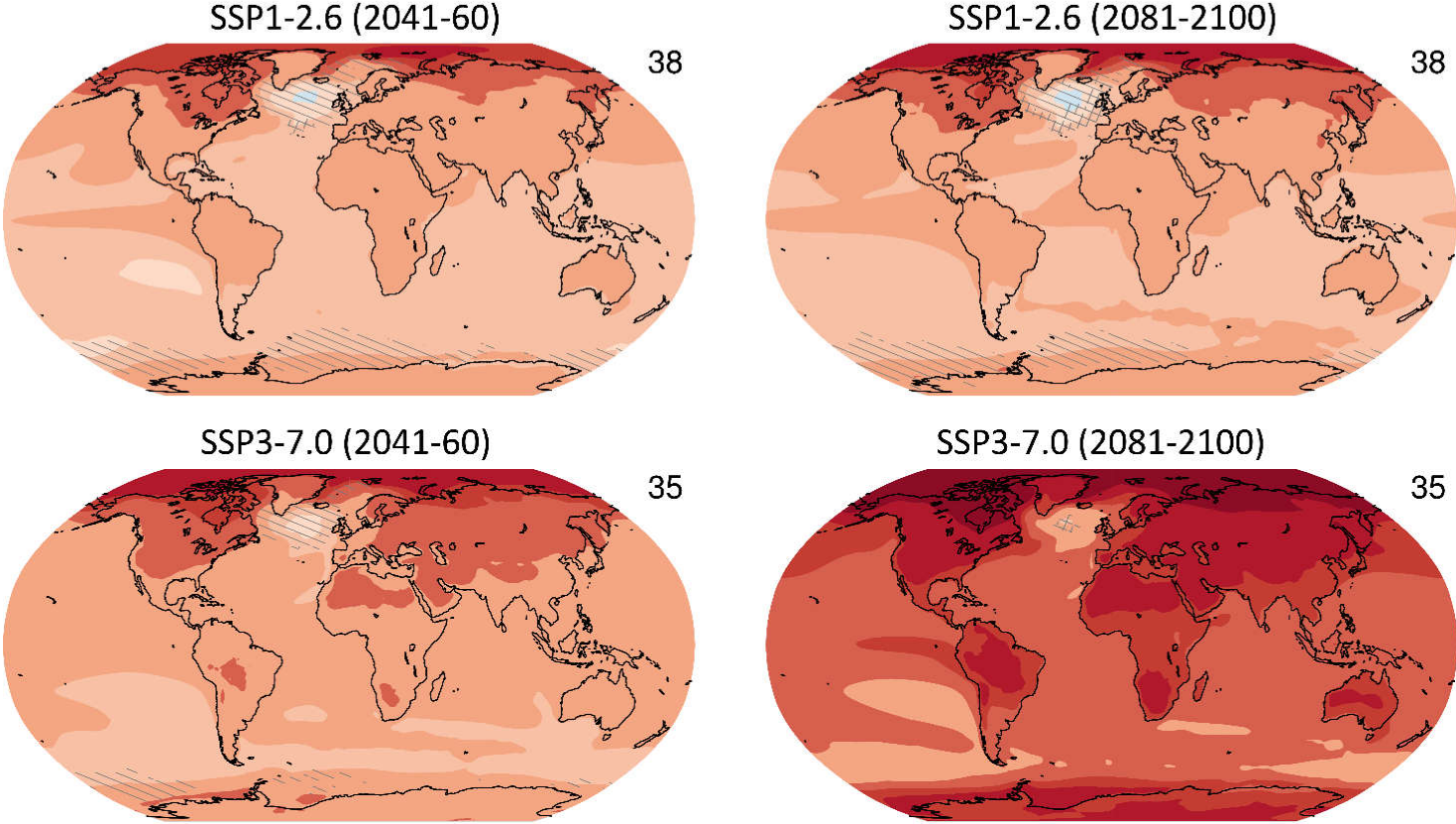


Mid- and long-term change of annual mean surface temperature

Figure 4.19: Mid- and long-term change of annual mean surface temperature. Displayed are projected spatial patterns of multi-model mean change in annual mean near-surface air temperature (°C) in 2041–2060 and 2081–2100 relative to 1995–2014 for (top) SSP1-2.6 and (bottom) SSP3-7.0. The number of models used is indicated in the top right of the maps. No overlay indicates regions where the change is robust and *likely* emerges from internal variability, that is, where at least 66% of the models show a change greater than the internal-variability threshold (see Section 4.2.6) and at least 80% of the models agree on the sign of change. Diagonal lines indicate regions with no change or no robust significant change, where fewer than 66% of the models show change greater than the internal-variability threshold. Crossed lines indicate areas of conflicting signals where at least 66% of the models show change greater than the internal-variability threshold but fewer than 80% of all models agree on the sign of change. Further details on data sources and processing are available in the chapter data table (Table 4.SM.1).



Annual mean temperature change

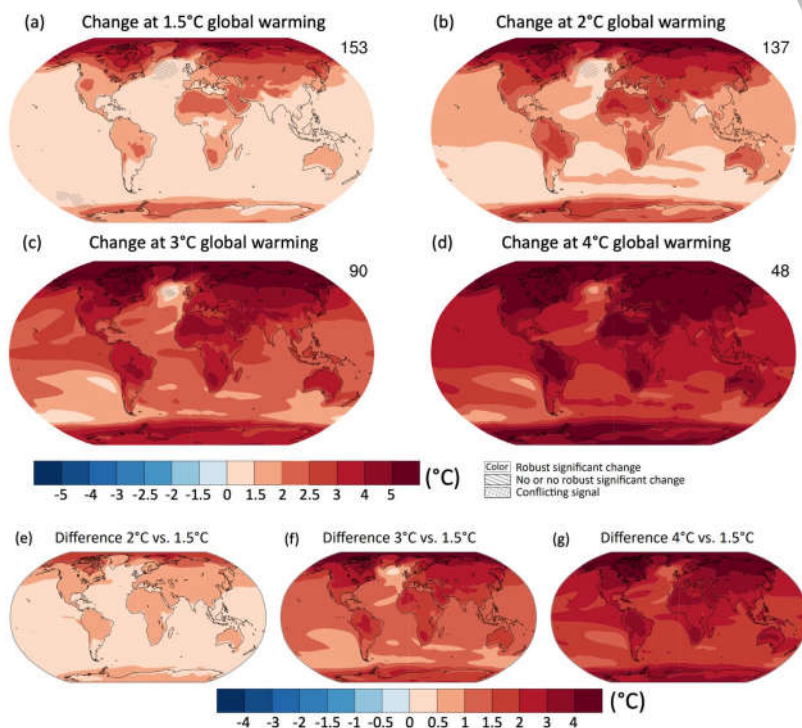


(°C)

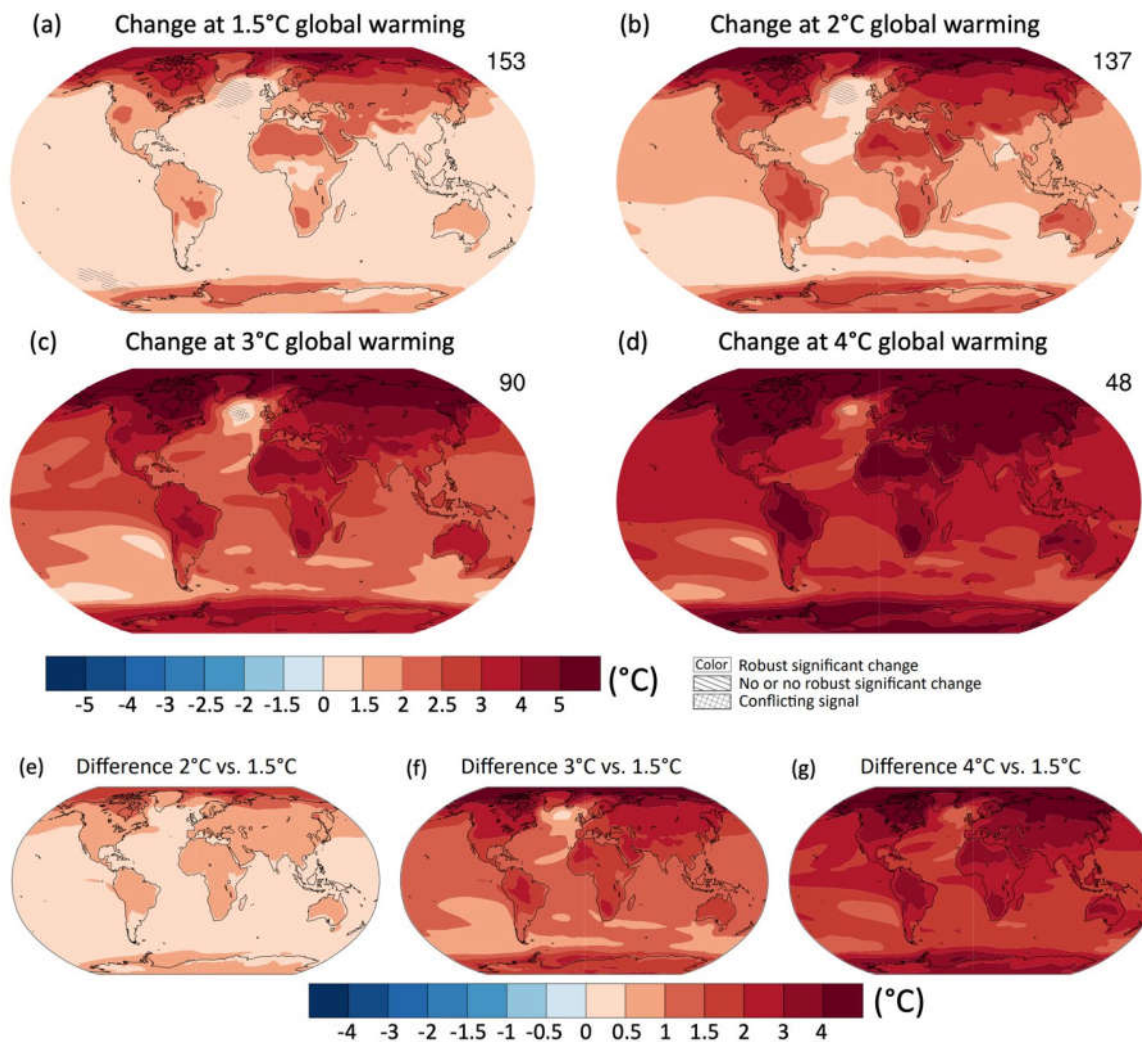
- Color Robust significant change
- No or no robust significant change
- Conflicting signal

Projected spatial patterns of change in annual average near-surface temperature (°C) at different levels of global warming.

Figure 4.31: Projected spatial patterns of change in annual average near-surface temperature (°C) at different levels of global warming. Displayed are (a–d) spatial patterns of change in annual average near-surface temperature at 1.5°C, 2°C, 3°C, and 4°C of global warming relative to the period 1850–1900 and (e–g) spatial patterns of differences in temperature change at 2°C, 3°C, and 4°C of global warming compared to 1.5°C of global warming. The number of models used is indicated in the top right of the maps. No overlay indicates regions where the change is robust and *likely* emerges from internal variability, that is, where at least 66% of the models show a change greater than the internal-variability threshold (see Section 4.2.6) and at least 80% of the models agree on the sign of change. Diagonal lines indicate regions with no change or no robust significant change, where fewer than 66% of the models show change greater than the internal-variability threshold. Crossed lines indicate areas of conflicting signals where at least 66% of the models show change greater than the internal-variability threshold but fewer than 80% of all models agree on the sign of change. Values were assessed from a 20-year period at a given warming level, based on model simulations under the Tier-1 SSPs of CMIP6. Further details on data sources and processing are available in the chapter data table (Table 4.SM.1).



IPCC 2021, Chap. 4



Difference of surface temperature change between JJA and DJF

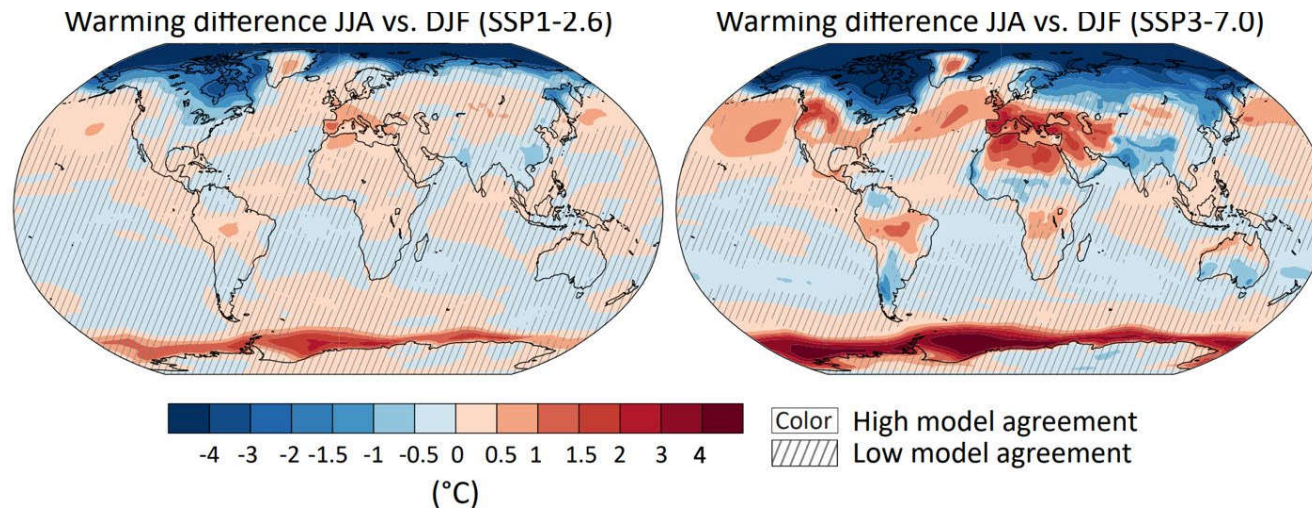
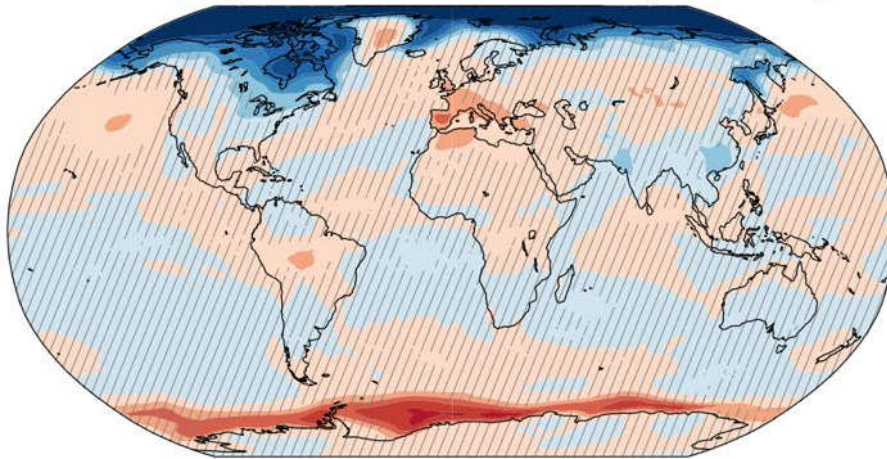


Figure 4.20: Difference of surface temperature change between JJA and DJF. Displayed are spatial patterns of multi-model mean difference in projected warming in JJA minus warming in DJF in 2081–2100 relative to 1995–2014 for (left) SSP1-2.6 and (right) SSP3-7.0. Diagonal lines mark areas where fewer than 80% of the models agree on the sign of change, and no overlay where at least 80% of the models agree. Further details on data sources and processing are available in the chapter data table (Table 4.SM.1).

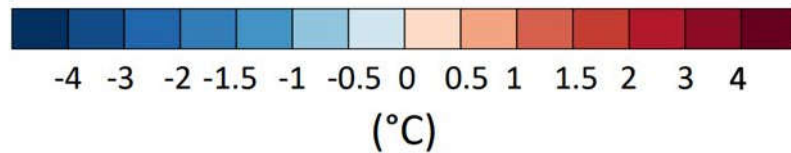
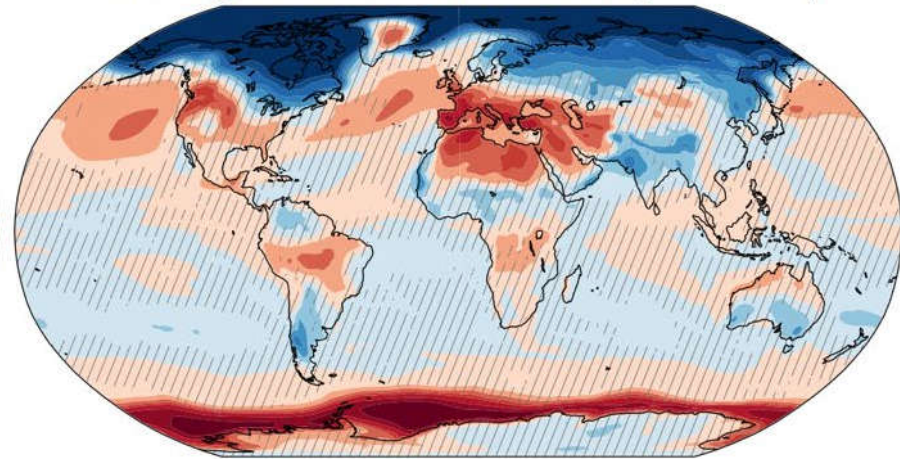


Difference of surface temperature change between JJA and DJF

Warming difference JJA vs. DJF (SSP1-2.6)



Warming difference JJA vs. DJF (SSP3-7.0)



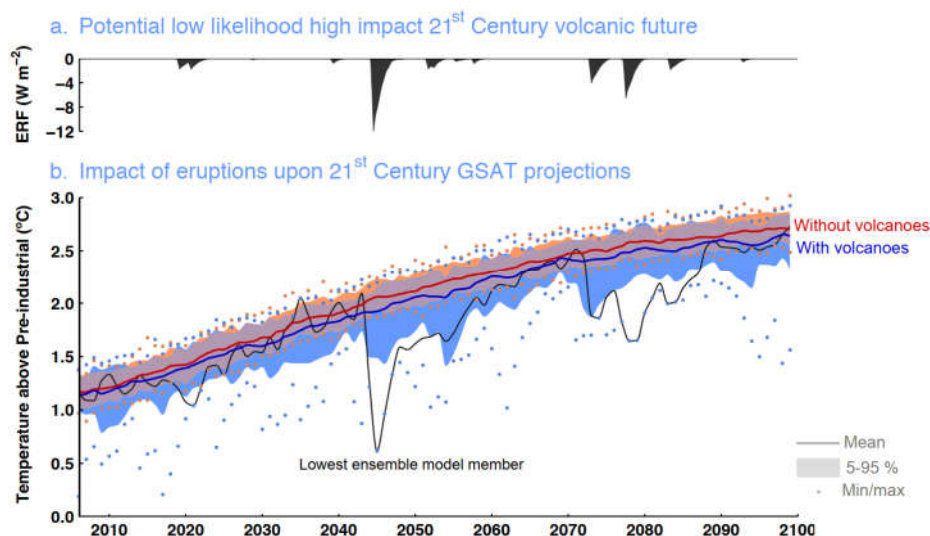
Color High model agreement
Hatched Low model agreement

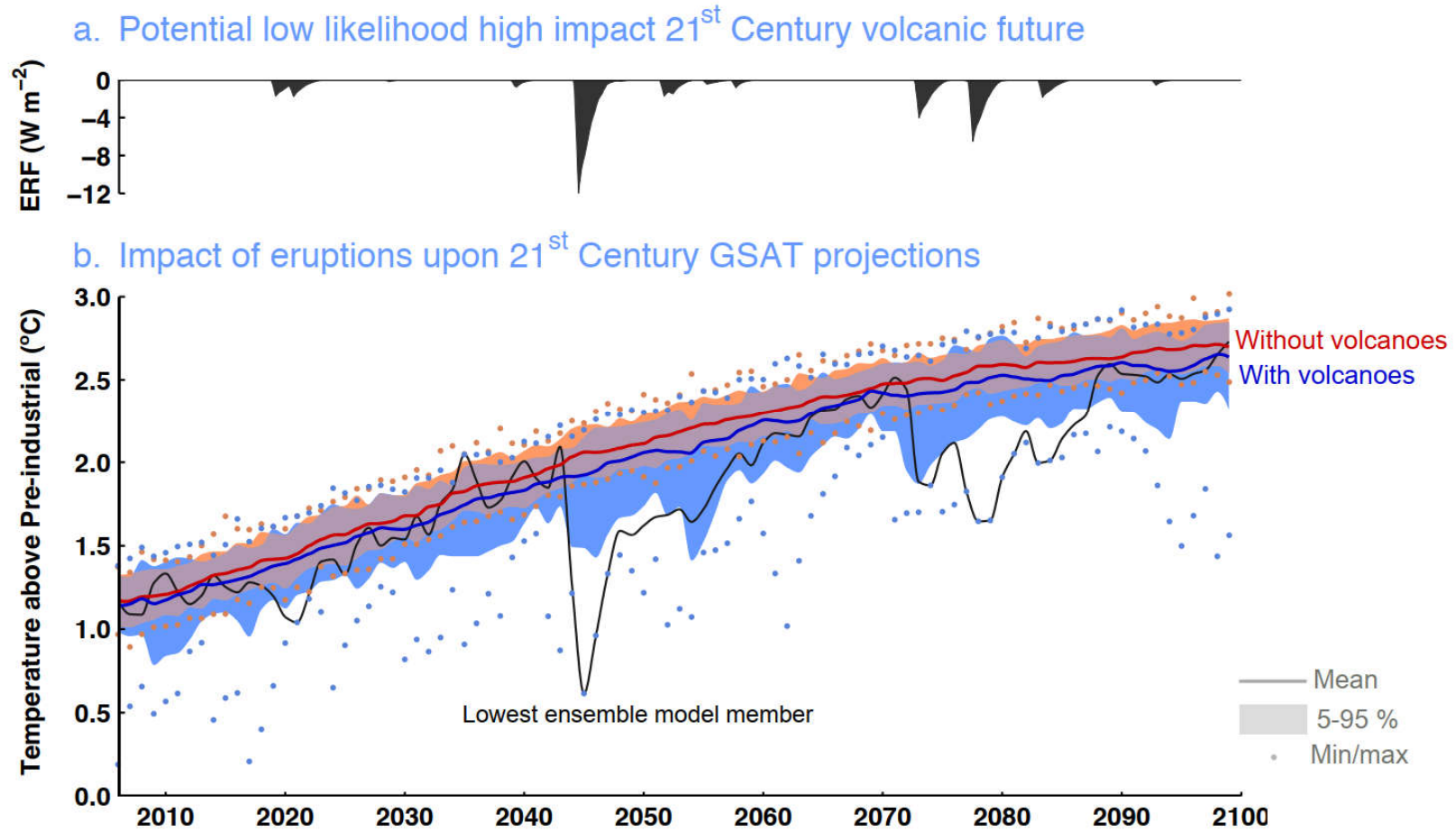


Potential impact of volcanic eruption on future global temperature change

Cross-Chapter Box 4.1, Figure 1: Potential impact of volcanic eruption on future global temperature change.

CMIP5 projections of possible 21st-century futures under RCP4.5 after a 1257 Samalas magnitude volcanic eruption in 2044, from Bethke et al. (2017). a, Volcanic ERF of the most volcanically active ensemble member, estimated from SAOD. b, Annual-mean GSAT. Ensemble mean (solid) of future projections including volcanoes (blue) and excluding volcanoes (red) with 5–95% range (shading) and ensemble minima/maxima (dots); evolution of the most volcanically active member (black). Data created using a SMILE approach with NorESM1 in its CMIP5 configuration. See Section 2.2.2 and Section 4.4.4 for more details. Further details on data sources and processing are available in the chapter data table (Table 4.SM.1).





IPCC 2021, Chap. 4



Statements in the Executive Summary

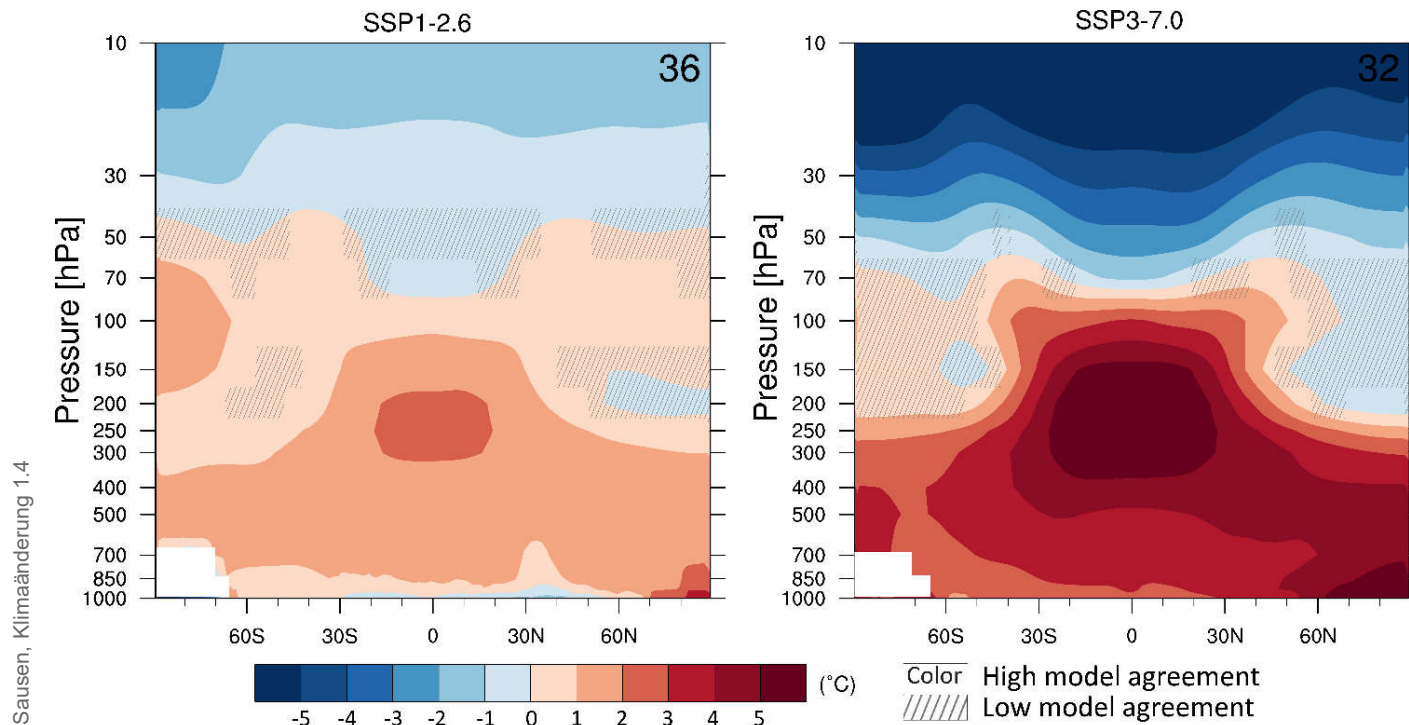
Temperature (8)

It is very likely that long-term lower-tropospheric warming will be larger in the Arctic than in the global mean. It is *very likely* that global mean stratospheric cooling will be larger by the end of the 21st century in a pathway with higher atmospheric CO₂ concentrations. It is *likely* that tropical upper tropospheric warming will be larger than at the tropical surface, but with an uncertain magnitude owing to the effects of natural internal variability and uncertainty in the response of the climate system to anthropogenic forcing. {4.5.1, 3.3.1.2}



Long-term change of annual and zonal mean atmospheric temperature

Figure 4.22: Long-term change of annual and zonal mean atmospheric temperature. Displayed are multi-model mean change in annual and zonal mean atmospheric temperature ($^{\circ}\text{C}$) in 2081–2100 relative to 1995–2014 for (left) SSP1-2.6 and (right) SSP5-8.5. The number of models used is indicated in the top right of the maps. Diagonal lines indicate regions where less than 80% of the models agree on the sign of the change and no overlay where 80% or more of the models agree on the sign of the change. Further details on data sources and processing are available in the chapter data table (Table 4.SM.1).



IPCC 2021, Chap. 4



